Research Article
doi.org/10.1002/slct.202500502

Chemistry Europe
European Chemical Societies Publishing

www.chemistryselect.org

Innovative Polymeric Sponges Loaded with Andiroba Oil and Cu(II) Complex: Synthesis, Characterization, Controlled Release, and Antimicrobial Activity

Jad Lorena F. Simplício,[a] Marinaldo V. de Souza Junior,[a] Jaqueline D. S. Barros,[a] João G. de Oliveira Neto,[a] Richard P. Dutra,[a] Adenilson O. dos Santos,[a] Francisco F. de Sousa,*[a, b] and Eliana B. Souto*[c]

Innovative polymeric sponges composed of andiroba oil (*Carapa guianensis* Aubl.) and 1,10-phenanthroline/Copper(II) crystalline complex, dispersed in sodium alginate and cellulose matrix were developed and their structural, vibrational, thermal, swelling, and antimicrobial properties characterized. The sponges were prepared by mixing the two polysaccharides with a fixed amount of andiroba oil following the addition of Cu(II) complex at different concentrations. The characterization of the samples by scanning electron microscopy and X-ray diffraction showed amorphous structures with several micropores. All sponges displayed water absorption capacity, with swelling increasing progressively over 120 min. Biodegradation assays were performed in phosphate buffer to evaluate sponges' degradation profile. Fourier transformed infrared spectra (FT-IR) revealed their main functional groups, together with bands assigned to interaction between Cu^{2+} ions and organic compounds. Differential scanning calorimetry analysis indicated compromised thermal stability attributed to sponges' dehydration. The sponges containing Cu(II) complex demonstrated controlled release of Cu^{2+} ions, with ions being released within the first 30 min. The antimicrobial effects were evaluated against strains of Gram-positive and Gram-negative bacteria, confirming the bactericidal activity of the developed sponges. These findings suggest that sponges composed of Cu^{2+} ions and andiroba oil have potential pharmaceutical applications to be used as a biomaterial with antimicrobial properties.

1. Introduction

Bacterial infections and drug resistance significantly impair the healing of severe chronic wounds, contributing to a high patients' morbidity and mortality.[1] Current treatment options are often limited in effectiveness and, in many cases, fail to fully restore the structure and function of damaged skin. This leads to complications, such as dehydration and infection, due to the need for frequent dressing changes and wound cleaning. Polysaccharide-based drug delivery systems have been proposed for wound healing,[2] as they offer the advantage of absorbing wound exudates and fluids without needing constant changing and cleaning, thereby minimizing the risk of further infections.[3] Therefore, polysaccharides have been widely effective in the treatment of difficult-to-heal skin ulcers, with the ability to largely "speed up" the regeneration process.[4]

Alginate and cellulose stand out as natural biopolymers with the ability to form biocompatible and biodegradable three-dimensional (3D) structures widely exploited for the development of innovative wound dressings.[2a] These materials can be processed into gels, polymeric blends, films, sponges, and porous membranes, with potential applications in tissue regeneration and wound dressings, and in the delivery of bioactive compounds, such as drugs, enzymes, cells and growth factors.[5]

Copper plays a crucial role in biochemistry and interaction with biomolecules.[6] Copper(II) complexes exhibit antacid, anti-inflammatory, antiviral, and antitumor properties.[6,7] These complexes interact with proteins and nucleic acids by complexing the metal ion with amino acids, interfering with the electron transport and oxygen metabolism. Cu(II) complexes also stand out as promising cytotoxic agents, inhibiting the proliferation of diseased cells and showing pharmacological effects.[8] Copper ions (Cu^{2+}) complexed with organic molecules (e.g., 1,10-phenanthroline) have demonstrated bactericidal, bacteriostatic, and fungistatic properties.[6,8] Phenanthroline is a bidentate ligand capable of forming stable complexes with metal ions, besides presenting properties, such as antifungal, antibacterial and antiviral activity.[9] Cu(II) complexes can eliminate or inhibit pathogenic growth, suppressing bacteria and fungi harmful to

[a] *J. L. F. Simplício, M. V. de S. Junior, J. D. S. Barros, J. G. de O. Neto, R. P. Dutra, A. O. dos Santos, F. F. de Sousa*
Center for Sciences of Imperatriz, Federal University of Maranhão–UFMA, Imperatriz, MA 65900-410, Brazil
E-mail: ffs@ufpa.br

[b] *F. F. de Sousa*
Institute of Exact and Natural Sciences, Federal University of Para–UFPA, Belém, PA 66075–110, Brazil

[c] *E. B. Souto*
UCD School of Chemical and Bioprocess Engineering, University College Dublin, Belfield, Dublin 4 D04 V1W8, Ireland
E-mail: eliana.souto@ucd.ie

© 2025 The Author(s). ChemistrySelect published by Wiley-VCH GmbH. This is an open access article under the terms of the Creative Commons Attribution License, which permits use, distribution and reproduction in any medium, provided the original work is properly cited.

© 2025 The Author(s). ChemistrySelect published by Wiley-VCH GmbH

Table 1. Composition of each developed sponge.

Sponge code	Sodium alginate/sodium carboxymethyl cellulose	$[Cu_2(mal)_2(phen)_2]$ $4H_2O$ 2MeOH	Andiroba oil
P	1.2%	–	–
PA	1.2%	–	1.96%
$PAC_{0.5}$	1.2%	0.5%	1.96%
$PAC_{1.0}$	1.2%	1.0%	1.96%
$PAC_{2.0}$	1.2%	2.0%	1.96%

human health.[6,10] However, these activities can be significantly enhanced if the complex material is loaded within a polymeric matrix, aiming at improving the complex stability and targeting.[11]

Oil-in-water nanoemulsions are thermodynamically unstable biphasic systems that can be produced from oils with pharmacological properties.[12] These oils can also be used to incorporate lipophilic compounds with antimicrobial and antioxidant properties.[13] The incorporation of these nanoemulsions into polymeric sponges has additional advantages, as their permeability to water vapor increases, facilitating better gas exchange and promoting more efficient moisture management, which are fundamental aspects for both skin health and the healing process itself.[14] In this way, the combination of polymers with nonvolatile oils and Cu^{2+} complexes can enhance the biological properties and result in a multifunctional material, capable of being adapted for specific biomedical applications, especially in the treatment of wounds.

Nonvolatile oils, often derived from natural sources, play a significant role in various industries, including food, cosmetics and pharmaceutics.[15] These oils are characterized by their high boiling points and low vapor pressures, making them stable and effective vehicles for the delivery of drugs.[16]

Andiroba oil, derived from the seeds of the *Carapa guianensis* tree, is traditionally used in Amazonian medicine for its anti-inflammatory, analgesic, antimicrobial, and antimalarial properties.[17] Andiroba oil is rich in oleic, palmitic, and linoleic acids, with oleic acid being the most abundant.[18] The presence of these fatty acids, along with myristic acid, contributes to the oil's therapeutic potential. Sustainable extraction methods enhance its economic viability, and its antioxidant properties further support its use in various industries.[19]

Paranhos et al.[20] reported that incorporating natural oils, such as copaiba oil, into chitosan-based polysaccharide matrices enhanced key wound dressing properties, including fluid absorption capacity and antimicrobial activity. These oil-polysaccharide composites offer multiple therapeutic advantages for wound healing applications, such as antimicrobial and anti-inflammatory effects, improved porosity, enhanced fluid management, and controlled release capabilities, collectively contributing to more efficient wound recovery. Ferreira et al.[21] incorporated andiroba oil also into chitosan-based polysaccharide matrices for the treatment of wounds. Their findings indicate that andiroba oil improves chitosan membranes' performance by promoting granulation tissue formation, tissue contraction, and epithelialization, while also increasing the material's hydrophobicity–a crucial factor for maintaining optimal wound moisture and facilitating cell regeneration. These combined effects create a more favorable environment for tissue repair, enhance healing efficiency, and reduce pain associated with wound dryness, highlighting the therapeutic potential of such oil-polysaccharide composites in wound care applications.

The present study aimed at producing innovative polymeric sponges based on andiroba oil (*Carapa guianensis* Aubl.) incorporating Cu^{2+} ions, and coated with a polymeric mixture of alginate and cellulose. Their structural, vibrational, thermal, and swelling properties of the obtained sponges were characterized for possible applications as an antimicrobial composite. Furthermore, biodegradation and controlled release experiments were conducted, showing optimal parameters for developing pharmaceutical products against pathogenic microorganisms.

2. Materials and Methods

2.1. Materials

Sodium carboxymethyl cellulose (MW = 250.208 g/mol, content: ≥99.5%, pH (1% solution): 6 to 8.5) and sodium alginate (MW = 198.00 g/mol, content: max 91.0%–106.0%, pH (1% solution): 5 to 8) were purchased from Sigma-Aldrich (St. Louis, MO, USA) and andiroba oil (*Carapa guianensis* Aubl.) sourced *in natura* was obtained from a local market. The reagents used to obtain the $[Cu_2(mal)_2(phen)_2]4H_2O{\bullet}2MeOH$ crystals were 1,10-phenanthroline (10 mmol) (Biosynth, Staad, Switzerland, purity 99.0%), Cu(II) nitrate trihydrate (10 mmol) (Sigma-Aldrich, St. Louis, MO, USA, purity ≥ 98%), maleic acid (10 mmol) (Sigma-Aldrich, St. Louis, MO, USA, purity 99.0%) and methanol (Biosynth, Staad, Switzerland, content 99.8%).

2.2. Synthesis of Copper Complex Crystals

The complex $[Cu_2(mal)_2(phen)_2]4H_2O{\bullet}2MeOH$ was crystallized as previously described by us, by slow evaporation method. Briefly, a methanolic solution of Cu(II) nitrate trihydrate was prepared, then 1,10-phenanthroline was slowly added to the methanolic solution of metal, keeping the mixture at 75 °C under constant stirring for about 1 h. An aqueous solution (10 mL) of maleic acid

© 2025 The Author(s). ChemistrySelect published by Wiley-VCH GmbH

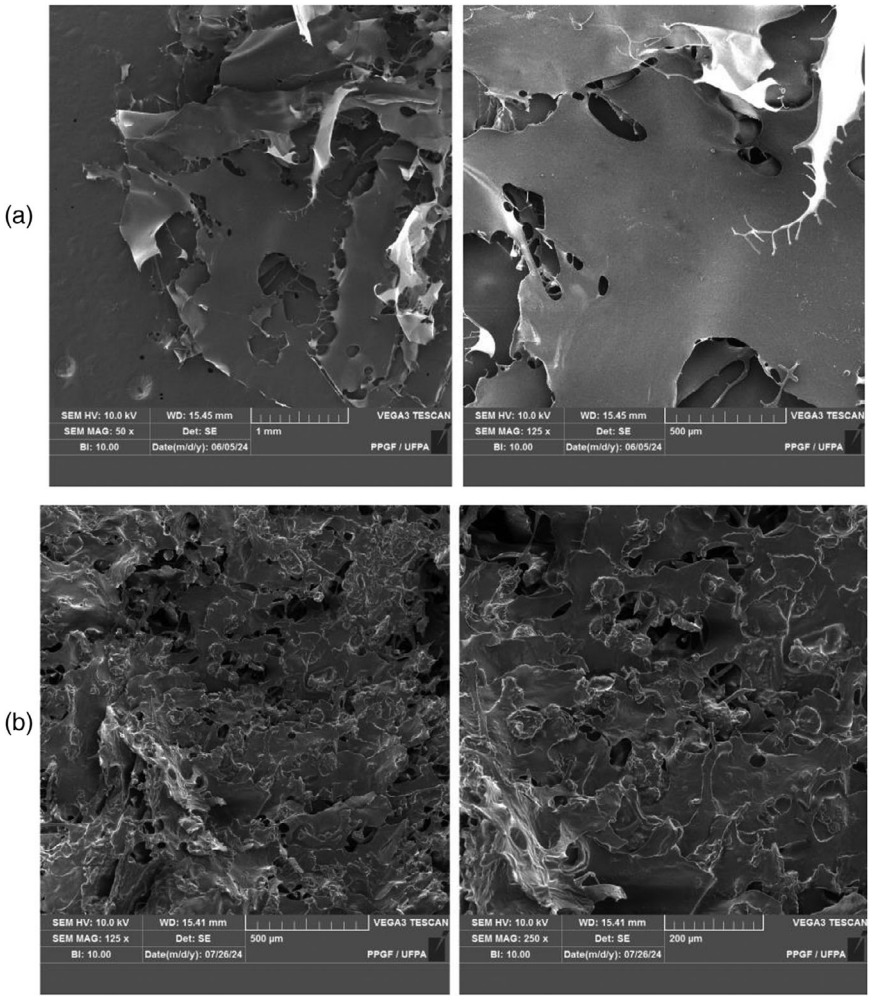


Figure 1. Scanning electron micrographs of sponge formulations (scale bar = 500 µm): a) P, b) PA, c) $PAC_{0.5}$, d) $PAC_{1.0}$, and e) $PAC_{2.0}$.

treated with NaOH (20 mmol) (Sigma-Aldrich, St. Louis, MO, USA, purity $\geq$ 98%) was slowly added to the above reaction mixture with continuous stirring for 30 min at 75 °C. The resulting solution was filtered through a filter paper with pores of 25 µm into a 75 mL beaker and subsequently covered with polyvinyl chloride (PVC, Sigma-Aldrich, St. Louis, MO, USA) film, where some holes were made, and then taken for storage in the crystal growth room at a temperature of 25 °C, to favor the slow evaporation of the solvent, until formation of crystals.

2.3. Synthesis of Sponges

Three 1.2% (w/v) base solutions containing sodium carboxymethyl cellulose and sodium alginate were first prepared. The crystalline powder $[Cu_2(mal)_2(phen)_2]4H_2O\bullet 2MeOH$ was added in concentrations of 0.5%, 1%, and 2% (w/w), respectively, to each of the three 1.2% (w/v) polymeric solutions. A volume of 1.96% of andiroba oil was then added, under continued stirring at 300 RPM for another 24 h (VELP Scientifica, Usmate, Italy) to obtain the nanoemulsions. Following this, the nanoemulsions were transferred to Petri dishes and cooled down at low temperatures (−4 °C for 24 h) before being freeze-dried in a TERRONI LS3000 Freeze Dryer (Lyotech, São Carlos, Brazil) at −40 °C for 24 h.

Five different sponges were produced, namely pure polymer of alginate and cellulose (P); polymer and andiroba oil (PA); polymer, andiroba oil and crystalline powder at a concentration of 0.5% ($PAC_{0.5}$); polymer, andiroba oil and crystalline powder at a concentration of 1% ($PAC_{1.0}$); polymer, andiroba oil and crystalline powder at a concentration of 2% ($PAC_{2.0}$). Their composition is summarized in Table 1.

2.4. Characterization Techniques

The morphology of the sponges was characterized by scanning electron microscopy (SEM) in a Tescan Vega3 SB equipment (Kohoutovice, Czech Republic). Samples were mounted on carbon tapes and coated with a thin gold/palladium layer (20 nm) to improve conductivity. The imaging was performed at low accelerating voltages (6–10 kV) to preserve sample integrity, and micrographs were recorded at different scales and magnifications to capture detailed surface morphology. The percentage

© 2025 The Author(s). ChemistrySelect published by Wiley-VCH GmbH

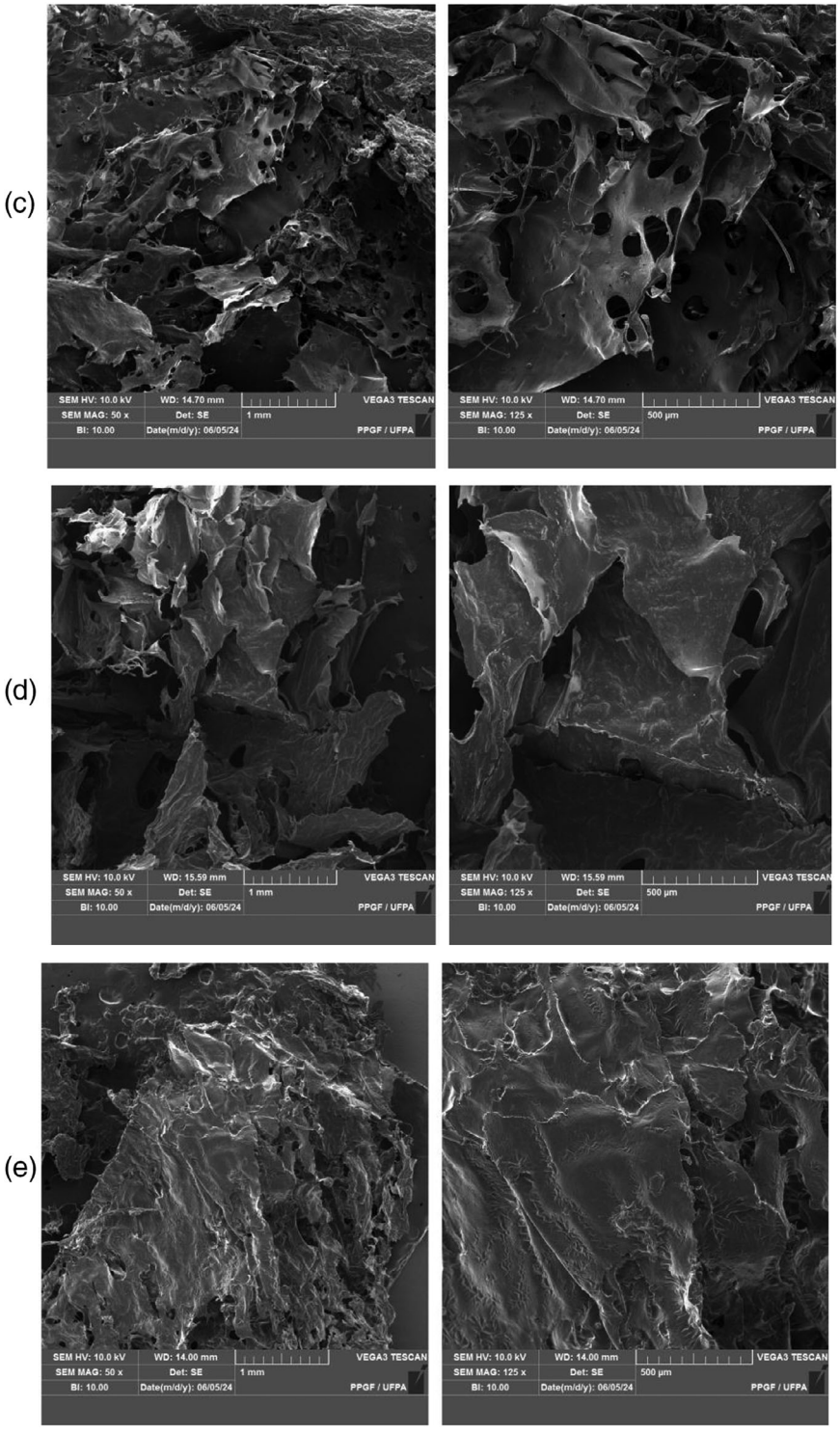


Figure 1. *Continued*

of porosity was determined by analyzing images obtained by optical microscopy using ImageJ software, which allows reliable quantification of pore area from binarized images.

To investigate the structural nature of polymeric sponges containing andiroba oil and Cu(II) complex, powder X-ray diffraction (PXRD) technique was performed in a PANalytical Empyrean diffractometer (Malvern PANalytical, Malvern, UK), operating with Cu-$K_{\alpha 1}$ radiation ($\lambda = 1.5418$ Å) at 40 kV and 40 MA. The data were collected over an angular range of 7 °–55 ° with a step of 0.02° per 2 s, at 27 °C.

Fourier transform infrared (FT-IR) spectroscopy was conducted to identify the functional groups in the sponges. Spectra were measured in transmission mode using a Bruker Vertex 70V spectrometer (Bruker, Billerica, Massachusetts, USA) in the

© 2025 The Author(s). ChemistrySelect published by Wiley-VCH GmbH

spectral range of 400 to 4000 cm^{-1}. An A225/Q Platinum Total Reflectance Attenuated (ATR) module and a wide 6 mm aperture RT-DLA TGS detector were used on the sample, allowing measurements over 400 cm^{-1} with a spectral resolution of 4 cm^{-1} for 100 scans. Baseline correction was systematically applied to all spectra to enhance data interpretation and ensure accurate band identification.

Differential scanning calorimetry (DSC) was used to analyze the thermal properties of the sponges. The measurement was performed on Shimadzu DSC-60 (Kyoto, Japan) equipment under a nitrogen atmosphere (100 mL/min) at a heating rate of 5 °C/min, in a temperature range from 25 °C to 300 °C.

2.5. Swelling and Biodegradation Tests

The water absorption capacity (deionized water was used as solvent) of the sponges was quantified by calculating the mass ratio of incorporated water (m_{water}) to the initial dry weight (m_{dry}) at various time intervals (0, 1, 3, 5, 10, 15, 30, 60, 90, and 120 min), as described in Equation (1):[22]

$$\text{Swelling} = \left(m_{water} - m_{dry}\right)/m_{dry} \quad (1)$$

The biodegradation behavior of the sponges was evaluated through gravimetric analysis by monitoring mass loss over time under simulated physiological conditions. Samples were immersed in phosphate-buffered saline (pH 7.4) at 37 °C under gentle stirring (50 RPM). At predetermined intervals (1, 30, 60, 90, and 120 min), specimens were removed, thoroughly rinsed with deionized water, dried to constant weight, and reweighed to determine residual mass. The degradation percentage was calculated using the Equation (2):

$$\text{Biodegradation}\,(\%) = (m_o - m_t)/m_o \quad (2)$$

where m_o is the initial dry mass and m_t is the dry mass at time t. Both experiments were performed in triplicate.

2.6. In Vitro Release Kinetics of Cu^{2+} Ions from Sponges

The release kinetics of Cu^{2+} ions from sponges was evaluated in phosphate buffer solution (pH 6.8) at 37 °C. Samples (≈0.2 g) were dispersed in 100 mL of phosphate buffer under constant stirring (360 RPM) for 120 min. Aliquots (2 mL) were collected at predetermined time points and analyzed using a Thermo Scientific Evolution 220 UV-Vis-NIR spectrophotometer (Waltham, MA, USA). Copper concentration was determined at 640 nm, corresponding to the characteristic absorption band of Cu^{2+} ions in solution, using a calibration curve ($R^2 = 0.9891$, coefficient of variation $< 3\%$).

2.7. Antibacterial Activity

The bactericidal activity of the sponges was evaluated using the disk diffusion method[23] to determine whether the bacteria were sensitive or resistant to the polymeric sponges containing andiroba oil and Cu(II) complex. The bacterial strains *Staphylococcus aureus* (ATCC 6538), *Escherichia coli* (ATCC 25922), *Pseudomonas aeruginosa* (ATCC 27853), and *Enterococcus faecalis* (ATCC 25923) were employed to assess the antimicrobial activity of the sponges. These strains were suspended in Mueller–Hinton broth (Kasvi, Minas Gerais, Brazil) for testing. The bacterial inoculum of each strain was prepared following the turbidity scale corresponding to bacterial growth in Mueller–Hinton broth of 1×10^8 CFU/mL compatible with a turbidity of 0.5 on the McFarland standard scale, obtaining absorbance in the range of 0.08–0.10 at 630 nm in a microplate spectrophotometer (BioTek Instruments, Winooski, Vermont, USA). The sponges were cut into 8.5 mm discs and placed on a plate containing Mueller–Hinton broth and incubated at 35 °C for 24 h. Each sample was tested in triplicate to ensure reproducibility. The area without bacterial growth around the sponges was considered as the zone of inhibition, indicating a potential antimicrobial effect.

2.8. Statistical Analysis

The bactericidal activity was assessed using mean ± standard deviation, with variance calculated to evaluate data dispersion. Statistical validation was performed to ensure result reliability and experimental reproducibility.

3. Results and Discussion

3.1. Structural Analysis via SEM and PXRD

Figure 1a–e shows the morphology and detailed microstructure of alginate-cellulose polymeric sponges incorporated with Cu^{2+} ions and andiroba oil. In Figure 1a, the structure of a sponge composed of polymers only (P sponge, Table 1) shows a slightly porous morphology; the mixture of two polymers can form interconnected networks when processed together with good mechanical stability.[24] The walls that form the edges of the pores were thin and of a relatively smooth surface, with few irregularities due to the interaction between the alginate and cellulose after the freeze-drying process. The morphology of the PA sponge (Figure 1b) exhibited a porous structure with characteristics that are typical of the biopolymers and aqueous emulsion. The presence of polymers suggests a matrix with high structural stability, whereas andiroba oil can influence the morphology, creating oily pores with a morphology typical of an oil-in-water emulsion.[24,25] The micrograph of sponges $PAC_{0.5}$, $PAC_{1.0}$, and $PAC_{2.0}$ (Figure 1c–e) shows structures with greater surface complexity and porosities. The polymeric matrix of alginate and cellulose, with the help of andiroba oil, creates a network that allows the incorporation of crystals containing Cu^{2+} ions.

© 2025 The Author(s). ChemistrySelect published by Wiley-VCH GmbH

Table 2. Percentage of porosity of sponges obtained by image analysis via ImageJ, analyzed by optical microscopy (500 µm scale).

Sample code	Percentage
P	50.520%
PA	61.424%
$PAC_{0.5}$	59.082%
$PAC_{1.0}$	52.865%
$PAC_{2.0}$	65.171%

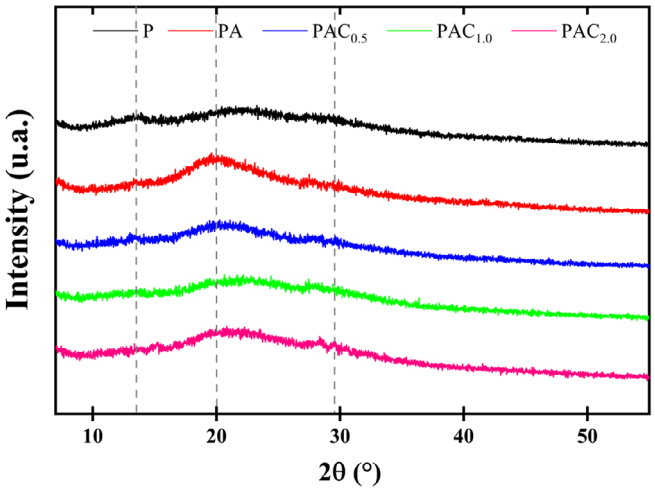


Figure 2. Diffractograms obtained for sponges P, PA, $PAC_{0.5}$, $PAC_{1.0}$, and $PAC_{2.0}$.

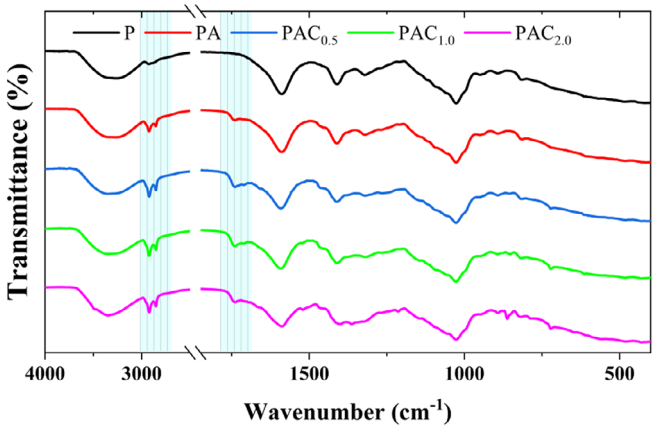


Figure 3. Experimental IR spectra of sponges P, PA, $PAC_{0.5}$, $PAC_{1.0}$, and $PAC_{2.0}$.

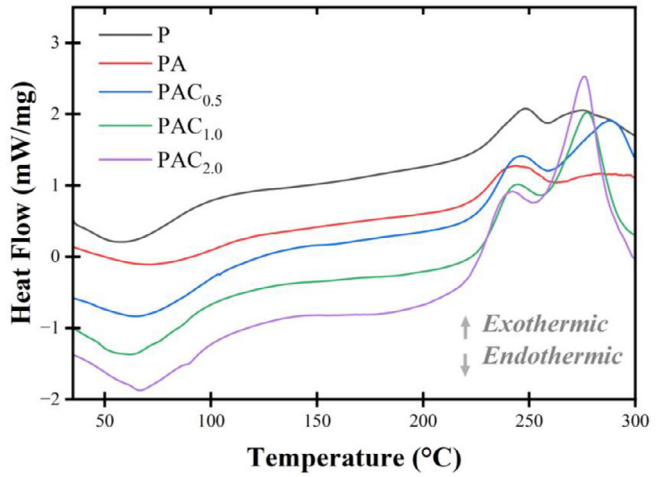


Figure 4. Heat flux of the sponges of sponges P, PA, $PAC_{0.5}$, $PAC_{1.0}$, and $PAC_{2.0}$.

This porous structure can favor a gradual release, from which the crystals can be released over time,[24] depending on the solubility in liquid medium and the diffusion of the crystals through the polymeric matrix pores.

Analysis of Table 2 (supported by Figure 1 at 500 µm scale) reveals distinct porosity trends among the sponge formulations. The control sponge P (without andiroba oil or copper crystals) exhibited the lowest porosity (50.520%) among all samples. Incorporation of andiroba oil alone significantly increased porosity to 61.424%, suggesting its role as an effective porogenic agent, likely through phase immiscibility with the polymer matrix or microchannel formation during processing. Interestingly, porosity variation with copper crystal concentration followed a nonlinear trend. At moderate concentrations ($PAC_{0.5}$ and $PAC_{1.0}$), copper crystals appeared to reduce porosity, potentially due to pore filling by the inorganic phase or matrix compaction effects. However, at the highest concentration ($PAC_{2.0}$), we observed a notable porosity increase, possibly indicating crystal-induced microstructural modifications that create larger or more distributed pores. This complex behavior suggests synergistic interactions between andiroba oil and copper crystals at higher concentrations, promoting structural instabilities that enhance the overall porosity.

Figure 2 shows the PXRD patterns of the polymeric sponges incorporated with andiroba oil and crystals containing Cu^{2+} ions in the angular range of $2\theta = 7$ ° to 55°. The diffractograms reveal the presence of three broad halos centered around $2\theta = 13$ °, $2\theta = 20$ °–22°, and $2\theta = 27$ °–29 °. The dashed lines indicate that the diffractogram of the sponge P (polymer of alginate and cellulose) shifted toward larger angles, suggesting that the material is more contracted and rigid due to interactions between the long monomeric chains of the alginate and cellulose macromolecules. In contrast, the diffractograms of the polymer combined with andiroba oil and crystalline grains at various concentrations (PA, $PAC_{0.5}$, $PAC_{1.0}$, and $PAC_{2.0}$) shifted toward smaller angles, indicating that the addition of these compounds causes an expansion or increased spacing between the monomeric chains of the polymer.

Furthermore, the absence of crystalline peaks in the XRD pattern indicates that the material has an amorphous structure, in other words, the interaction between the chemical groups (unsaturated fatty acids,[19a] organic and inorganic molecules) does not provide a long-range atomic ordering nature.

© 2025 The Author(s). ChemistrySelect published by Wiley-VCH GmbH

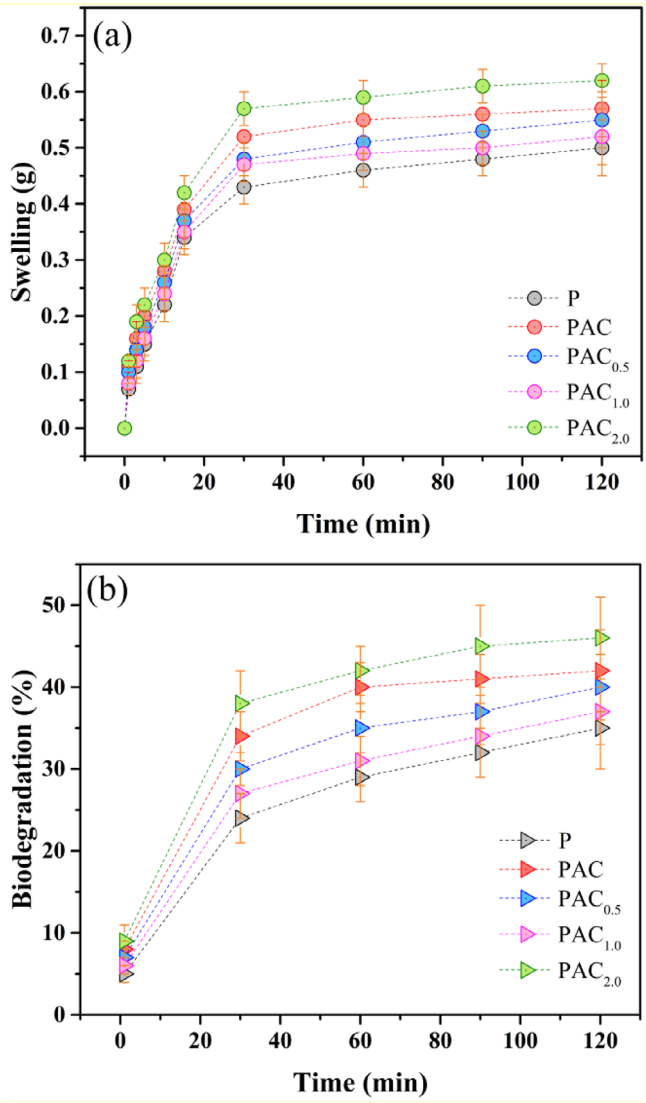


Figure 5. a) Swelling degree determined by the measurement of the water absorption capacity for the synthesized sponges as a function of time. b) Biodegradation profile for sponges under simulated physiological conditions over time.

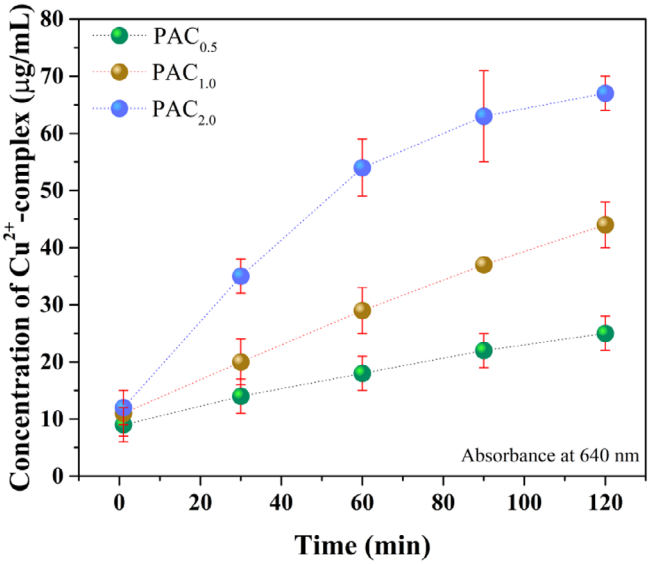


Figure 6. Release kinetic curves for the $PAC_{0.5}$, $PAC_{1.0}$, and $PAC_{2.0}$ sponges in phosphate buffer solution.

3.2. Infrared Vibrational Spectroscopy

In addition to structural characterizations, vibrational analyses are of great importance in materials science because these provide detailed information about the chemical composition and functional groups present in the polymer matrix.[26]

The IR absorption spectra of the sponges incorporated with andiroba oil and crystalline grains were analyzed for each formulation, as shown in Figure 3. In the spectra of P, PA, $PAC_{0.5}$, $PAC_{1.0}$, and $PAC_{2.0}$, a broad band is observed between wavenumbers 3746 and 3020 cm^{-1}, corresponding to the stretching vibration of OH groups (present in both cellulose and alginate), as well as the H_2O and methanol molecules present in the crystals. In the spectra containing andiroba oil, the bands near 2925 and 2852 cm^{-1} are attributed to stretching vibrations of C—H and C—O bonds, and to in-plane deformations of the CH—OH bonds, possibly related to the triglycerides belonging to andiroba oil which is rich in fatty acids,[27] and compounds related to crystalline grains.[25] In the same region of the P spectrum, only a minor shoulder is observed, corresponding to the vibrations of the polymeric carbon chains.[2a,28]

The spectra of PA, $PAC_{0.5}$, $PAC_{1.0}$, and $PAC_{2.0}$ show bands related to the stretching of the C═C double bond and of carbonyl unit (C═O) at approximately 1743 and 1600 cm^{-1}, with similar characteristics because of the presence of fatty acids in andiroba oil. Between 1500 and 1200 cm^{-1} significant differences are observed, highlighting the interaction of the crystalline grains with the polymer due to the deformation of the bands as the concentration of crystals increases. Wavenumbers around 1200 and 1000 cm^{-1} are associated with vibrations of C—O—C bonds, typical of polysaccharides.[29]

These observations suggest an increasing interaction between andiroba oil, the alginate/cellulose matrix, and the copper crystals, especially with increasing crystal concentration.

3.3. Differential Scanning Calorimetry (DSC)

Figure 4 shows the DSC thermogram of the sponges P, PA, $PAC_{0.5}$, $PAC_{1.0}$, and $PAC_{2.0}$, highlighting both endothermic and exothermic events. The first endothermic events are related to the enthalpy of vaporization of the water molecules that were absorbed by the sponges during the storage time, with the following values: 84 kJ/mol (P), 136 kJ/mol (PA), 108 kJ/mol ($PAC_{0.5}$), 131 kJ/mol ($PAC_{1.0}$), and 180 kJ/mol ($PAC_{2.0}$). An increase in enthalpy values is observed from formulation based only on polymers (P sponges) to the formulation containing 2% of $Cu_2(mal)_2(phen)_2]4H_2O•2MeOH$ ($PAC_{2.0}$ sponges). This happens in hydrophilic polymers, such as cellulose and alginate, where water tends to form strong hydrogen bonds with hydroxyl (OH) and carboxylate (COO^-) groups. $PAC_{2.0}$ sponges, on the other hand, have a higher number of molecules, favoring a greater

© 2025 The Author(s). ChemistrySelect published by Wiley-VCH GmbH

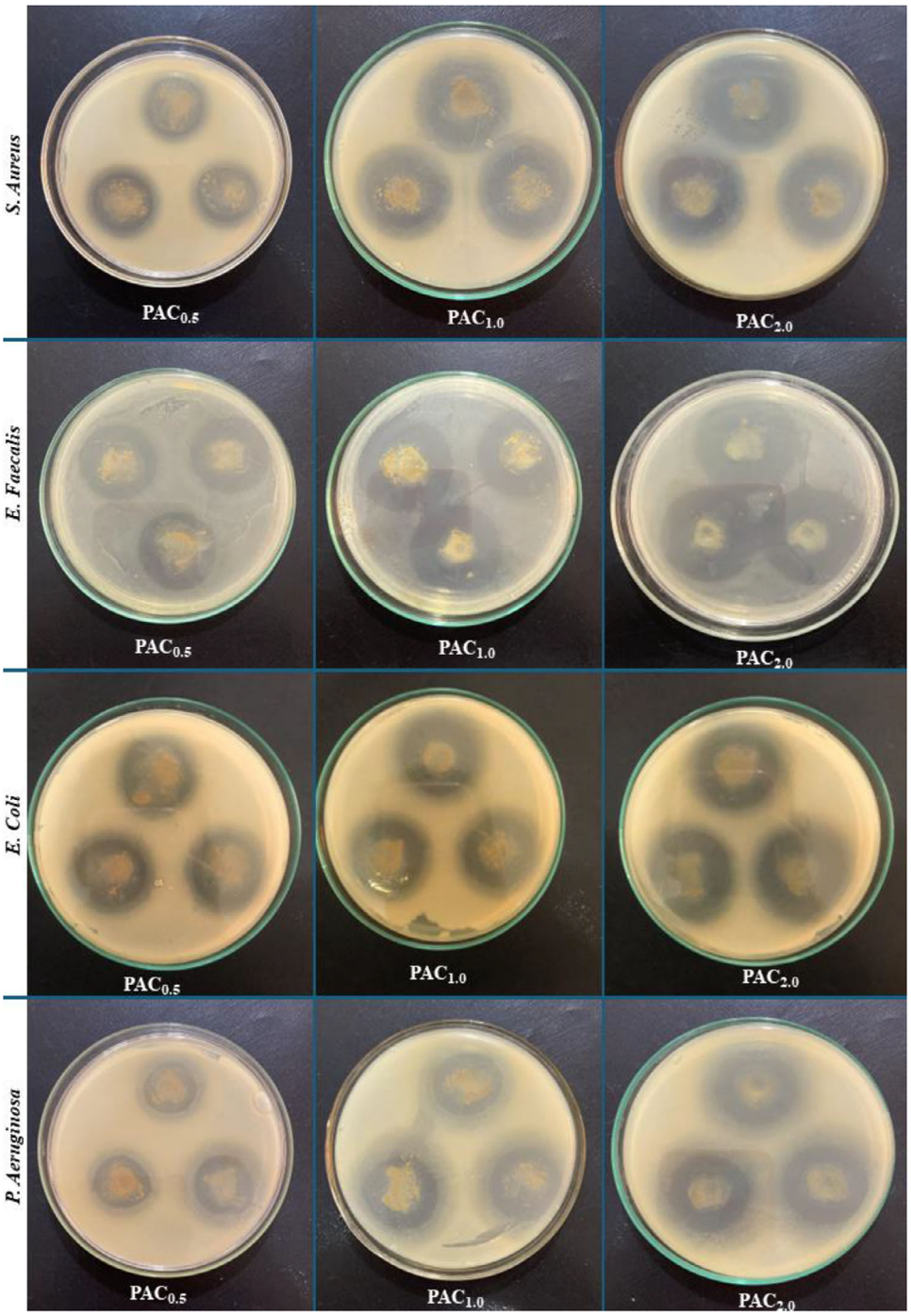


Figure 7. In vitro antibacterial inhibition zones of P, PA, $PAC_{0.5}$, $PAC_{1.0}$, and $PAC_{2.0}$, against Gram-positive (*S. aureus* and *E. faecalis*) and Gram-negative (*E. coli* and *P. aeruginosa*).

amount of hydrogen bonds and consequently increasing the network energy between chemical species. These interactions (strong chemical bonds, i.e., the covalent bonds belonging to the complex) require more energy to break, which increases the enthalpy of vaporization compared to water that is not bound. Therefore, the stronger the bond between water and the polymer, the greater the enthalpy of vaporization, as more energy will be required to release water from the polymeric matrix.[30]

The two exothermic events indicate the partial decomposition of the polymeric matrix, occurring within the following temperature ranges: P sponge at 247 °C and 275 °C; PA sponge at 244 °C and 289 °C; $PAC_{0.5}$: 246 °C and 288 °C; $PAC_{1.0}$: 244 °C and 277 °C; $PAC_{2.0}$: 241 °C and 276 °C. These exothermic events involve the breakdown of the monomeric chains of alginate and cellulose, as well as the organic molecules belonging to the crystals and andiroba oil.

© 2025 The Author(s). ChemistrySelect published by Wiley-VCH GmbH

Table 3. Mean, standard deviation and variance of the diameters (mm) from bacterial inhibition zones of the sponges against Gram-positive and Gram-negative bacteria.

Gram-positive	Statistical data	P	PA	$PAC_{0.5}$	$PAC_{1.0}$	$PAC_{2.0}$
S. aureus ATCC 6538	Average	0	0	15.0 mm	18.3 mm	23.3 mm
	Standard deviation	0	0	0.41 mm	0.88 mm	1.67 mm
	Variance	0	0	0.11 mm^2	0.51 mm^2	1.90 mm^2
E. faecalis ATCC 29212	Average	0	0	20.7 mm	26.7 mm	29.6 mm
	Standard deviation	0	0	0.50 mm	1.05 mm	0.74 mm
	Variance	0	0	0.16 mm^2	0.74 mm^2	0.36 mm^2
Gram-negative	Statistical data	P	PA	$PAC_{0.5}$	$PAC_{1.0}$	$PAC_{2.0}$
E. coli ATCC 25922	Average	0	0	19.1 mm	21.9 mm	22.8 mm
	Standard deviation	0	0	1.32 mm	1.16 mm	1.27 mm
	Variance	0	0	1.17 mm^2	0.90 mm^2	1.08 mm^2
P. aeruginosa ATCC 27853	Average	0	0	11.1 mm	18.7 mm	19.3 mm
	Standard deviation	0	0	0.85 mm	1.21 mm	0.41 mm
	Variance	0	0	0.48 mm^2	0.98 mm^2	0.11 mm^2

3.4. Swelling Behavior and Biodegradation Studies

Figure 5a displays the swelling behavior of the sponges in an aqueous medium as a function of time. As observed, the PAC sample exhibits higher swelling values than the P sample at all time intervals, confirming that andiroba oil acts as a porogenic agent (consistent with the SEM results discussed earlier), thereby enhancing liquid absorption. For the sponges containing Cu(II) complexes, reduced swelling was observed in $PAC_{0.5}$ and $PAC_{1.0}$ compared to PAC, suggesting partial pore filling and matrix compaction at 0.5% and 1% crystal concentrations. In contrast, higher crystal loading (2%, $PAC_{2.0}$) resulted in increased swelling, likely due to additional pore formation or structural modifications induced by crystal aggregation. In general, all sponges reached ~80% of maximum swelling within the first 30 min, followed by gradual saturation until 120 min, showing a kinetic profile typical of controlled diffusion systems, which aligns with their potential application as wound dressings.

Figure 5b presents the biodegradation kinetics under simulated physiological conditions as a function of time. The results show that the PAC sample degraded faster than the control P at all evaluated time points, suggesting that andiroba oil enhances hydrolytic cleavage of the polymer matrix. This observation aligns with its porogenic role, as evidenced by SEM and swelling studies, which increases the effective surface area for degradation. For $PAC_{0.5}$ and $PAC_{1.0}$, intermediate degradation rates were observed (≈40% and 37% at 120 min, respectively), attributed to partial pore occlusion by Cu(II) crystals, which slightly delayed saline-mediated degradation. In contrast, $PAC_{2.0}$ exhibited accelerated degradation (≈46% at 120 min), likely due to structural defects and enlarged pores caused by excessive crystal loading (2%), facilitating faster breakdown. All sponges displayed rapid initial degradation (≈70% within 30 min), followed by a decelerated phase, a pattern characteristic of surface-eroding biomaterials. The strong correlation between swelling ($PAC_{2.0}$: 0.62 g) and biodegradation (≈46%) highlights interconnected porosity-degradation mechanisms. This synergistic behavior is particularly advantageous for wound dressing applications, where controlled fluid absorption and timed degradation are critical for optimal performance.

3.5. Simulated Controlled Release

To investigate the controlled release of Cu^{2+} ions from $PAC_{0.5}$, $PAC_{1.0}$, and $PAC_{2.0}$ spheres, the samples were evaluated for their release kinetics in a liquid medium (phosphate buffer) over 120 min (Figure 6). For all three samples, a significant increase in Cu^{2+} ion concentration was observed over time, particularly within the first 60 min. Upon comparison, it was found that the sample with the highest percentage of dispersed crystals ($PAC_{2.0}$) reached the highest maximum concentration of Cu^{2+} ions in the medium (65 ± 3 mg/mL), followed by $PAC_{1.0}$ (40 ± 4 mg/mL) and $PAC_{0.5}$ (18 ± 3 mg/mL). These results indicate highly beneficial behavior from a clinical perspective, as the sponges containing the Cu(II) complex help maintain therapeutic concentrations of Cu^{2+} ions in the liquid medium, ensuring a controlled release profile.

3.6. Bactericidal Activity

To further complement the physicochemical analysis, a qualitative method was utilized to evaluate the bactericidal activity of the sponges. Figure 7 shows the in vitro antibacterial inhibition zones for sponges P, PA, $PAC_{0.5}$, $PAC_{1.0}$, and $PAC_{2.0}$, against Gram-

© 2025 The Author(s). ChemistrySelect published by Wiley-VCH GmbH

positive (*S. aureus* and *E. faecalis*) and Gram-negative (*E. coli* and *P. aeruginosa*) bacteria.

Table 3 depicts the statistical data of bacterial inhibition (halo diameter in mm) for the five sponges, as well as the statistical data of mean, standard deviation and variance. The results show that P (alginate/cellulose) and PA (polymer with oil) sponges exhibited no antibacterial activity.[31] The diameter of the inhibition zones of the sponges increased with the increase of the concentration of $[Cu_2(mal)_2(phen)_2]4H_2O•2MeOH$ (Figure 7 and Table 3). The $PAC_{2.0}$ concentration was the most effective against Gram-positive bacteria, presenting the largest inhibition halos for *S. aureus* (23.3 mm) and *E. faecalis* (29.6 mm). When interacting with the strains, the sponges can penetrate the bacterial membrane due to their solubility; the complex and its constituents could undergo ligand exchange processes, allowing the complex to interact with biomolecules within the pathogenic cells. This interaction could disrupt normal cellular processes, further supporting the antibacterial action of the sponge.

These data indicate that the incorporation of crystalline grains of the Cu(II) complex and andiroba oil into polymeric matrices can significantly enhance their effect for therapeutic use as antibacterial agents.

4. Conclusions

The sponges were successfully obtained by the freeze-drying technique at −40 °C. SEM and XRD analyses revealed that the addition of crystals to the alginate, cellulose, and andiroba oil matrix resulted in a structure with greater surface complexity and porosity, exhibiting an amorphous structural pattern. The IR spectra identified the key vibrational modes associated with the chemical composition and functional groups in the sponges, such as the stretching of OH, CH, CO, C═C and C═O. Thermal analysis showed an increase in the vaporization enthalpy values of H_2O molecules, attributed to the strong interactions between water and the polymeric matrix. Additionally, the combined data of swelling degree, biodegradation, and modified Cu^{2+} release, placing the sponges $PAC_{0.5}$, $PAC_{1.0}$, and $PAC_{2.0}$ as promising candidates for advanced wound dressings, where tailored material properties are pivotal for therapeutic efficacy. Moreover, antimicrobial studies demonstrated that the $PAC_{0.5}$, $PAC_{1.0}$, and $PAC_{2.0}$ sponges exhibited effective inhibition zones, confirming their antimicrobial properties. Our findings open perspectives for further studies by proposing the developed sponges as biomaterials with antimicrobial activity as adjuvants of healing processes.

Acknowledgments

The authors thank the support received from the Brazilian agencies CNPq, CAPES (finance code 001) and FAPEMA and from the University College Dublin Obrss Research Scheme fund 2024–2027 (83965-NP/R28429).

Conflict of Interests

The authors declare no conflict of interest.

Author Contributions

All authors actively contributed to the conceptualization, design of the study, methodology, validation, formal analysis, investigation, data curation and validation, literature review, software management, resources and facilities, writing—original draft preparation, writing—review and editing, project administration, supervision and funding acquisition. All authors have made a substantial contribution to the work.

Data Availability Statement

The data that support the findings of this study are available from the corresponding author upon reasonable request.

Keywords: Andiroba oil · Controlled release and bacterial inhibition · Cu^{2+} complex · Polymeric matrix

[1] a) B. M. A. d. B. Buriti, P. L. B. Figueiredo, M. F. Passos, J. K. R. da Silva, *Pharmaceuticals* **2024**, *17*, 897; b) J. G. de Oliveira Neto, J. A. O. Rodrigues, J. R. Viana, J. D. S. Barros, M. R. Lage, F. F. de Sousa, R. P. Dutra, E. B. Souto, A. O. dos Santos, *J. Mol. Liq.* **2024**, *403*, 124846.
[2] a) Y. Wen, B. Yu, Z. Zhu, Z. Yang, W. Shao, *Polymers* **2020**, *12*, 1926; b) V. A. Amaral, V. L. Santana, E. S. Lisboa, F. S. Martins, M. V. Chaud, R. L. C. de Albuquerque-Junior, W. Santana, C. Santos, A. de Jesus Santos, J. C. Cardoso, E. B. Souto, P. Severino, *Drug Deliv. Transl. Res.* **2025**, *15*, 1376–1392; c) H. Zhang, X. Lin, X. Cao, Y. Wang, J. Wang, Y. Zhao, *Bioactive Mater.* **2024**, *33*, 355–376.
[3] M. d. C. Aranha, L. M. R. Alencar, E. B. Souto, D. T. Kamei, A. M. Lopes, *Pharmaceuticals* **2024**, *17*, 1177.
[4] G. Tan, L. Wang, W. Pan, K. Chen, *Int. J. Nanomed.* **2022**, *17*, 3913–3931.
[5] a) M. Liu, J. Jin, X. Zhong, L. Liu, C. Tang, L. Cai, *Heliyon* **2024**, *10*, e35014; b) M. Nardini, S. Perteghella, L. Mastracci, F. Grillo, G. Marrubini, E. Bari, M. Formica, C. Gentili, R. Cancedda, M. L. Torre, M. Mastrogiacomo, *Pharmaceutics* **2020**, *12*.
[6] J. A. O. Rodrigues, N. S. Kiran, A. Chatterjee, B. G. Prajapati, N. Dhas, A. O. dos Santos, F. F. de Sousa, E. B. Souto, *Biochem. Pharmacol.* **2025**, *231*, 116644.
[7] B.-L. Fei, W. Li, W.-S. Xu, Y.-G. Li, J.-Y. Long, Q.-B. Liu, K.-Z. Shao, Z.-M. Su, W.-Y. Sun, *J. Photochem. Photobiol., B* **2013**, *125*, 32–41.
[8] J. G. de Oliveira Neto, J. R. Viana, K. R. Abreu, A. L. A. Butarelli, A. P. A. dos Santos, M. R. Lage, F. F. de Sousa, E. B. Souto, A. O. dos Santos, *J. Mol. Struct.* **2025**, *1321*, 139757.
[9] a) A. Bencini, V. Lippolis, *Coord. Chem. Rev.* **2010**, *254*, 2096–2180; b) K. Molčanov, M. Jurić, B. Kojić-Prodić, *Dalton Trans.* **2014**, *43*, 7208–7218.
[10] W. O. Pereira, J. G. Oliveira Neto, J. R. Viana, G. G. C. Carvalho, C. Pessoa, M. R. Lage, A. S. Reis, F. F. de Sousa, A. O. dos Santos, *J. Mater. Sci.* **2024**, *59*, 9502–9518.
[11] J. G. Oliveira Neto, L. A. Cavalcante, E. S. Gomes, A. O. Dos Santos, F. F. Sousa, F. Mendes, A. A. M. Macêdo, *Polym. Eng. Sci.* **2020**, *60*, 71–77.
[12] G. Kaur, C. Panigrahi, S. Agarwal, A. Khuntia, M. Sahoo, *Food Phys.* **2024**, *1*, 100024.
[13] A. Mushtaq, S. Mohd Wani, A. R. Malik, A. Gull, S. Ramniwas, G. Ahmad Nayik, S. Ercisli, R. Alina Marc, R. Ullah, A. Bari, *Food Chem.: X* **2023**, *18*, 100684.
[14] M. Sufiyan, P. Kushwaha, M. Ahmad, P. Mandal, K. K. Vishwakarma, *AAPS PharmSciTech* **2024**, *25*, 137.
[15] K. W. Chan, M. Ismail, *Food Chem.* **2009**, *114*, 970–975.

© 2025 The Author(s). ChemistrySelect published by Wiley-VCH GmbH

[16] N. J. Sadgrove, G. F. Padilla-González, O. Leuner, I. Melnikovova, E. Fernandez-Cusimamani, *Front. Pharmacol.* **2021**, *12*, https://doi.org/10.3389/fphar.2021.740302.
[17] C. L. Porfírio-Dias, K. M. Melo, C. E. M. C. Bastos, T. A. A. Ferreira, L. F. C. Azevedo, H. L. Salgado, A. S. Santos, J. D. Rissino, C. Y. Nagamachi, J. C. Pieczarka, *J. Appl. Toxicol.* **2020**, *40*, 1060–1066.
[18] A. Q. Alves, V. A. da Silva Jr., A. J. S. Góes, M. S. Silva, G. G. de Oliveira, I. Bastos, A. G. de Castro Neto, A. J. Alves, *Advances in Skin & Wound Care* **2019**, *32*, 1–8.
[19] a) Z. Novello, J. Scapinello, J. D. Magro, G. Zin, M. D. Luccio, M. V. Tres, J. V. Oliveira, *Ind. Crops Prod.* **2015**, *76*, 697–701; b) C.-g. Zhang, C.-x. Zhao, Z. Ma, D.-y. Yan, *J. Coord. Chem.* **2000**, *52*, 87–95.
[20] S. B. Paranhos, E. D. S. Ferreira, C. A. A. Canelas, S. P. A. da Paz, M. F. Passos, C. E. F. da Costa, A. C. R. da Silva, S. N. Monteiro, V. S. Candido, *Polymers (Basel)* **2021**, *14*, 35.
[21] E. d. S. Ferreira, S. B. Paranhos, S. P. A. da Paz, C. A. d. A. Canelas, L. A. S. d. Nascimento, M. F. Passos, A. C. R. da Silva, S. N. Monteiro, M. V. d. S. Paula, V. S. Candido, *Polymers (Basel)* **2024**, *14*, 1105.
[22] J. G. O. de Neto, K. R. Abreu, O. C. Da Silva Neto, J. D. de Oliveira, A. O. Dos Santos, E. B. Souto, *ChemistrySelect* **2025**, *10*, e202404594.
[23] J. G. de Oliveira Neto, M. V. Souza Junior, A. P. Ayala, C. E. S. Nogueira, E. B. Souto, A. O. dos Santos, F. F. de Sousa, *Cryst. Growth Des.* **2024**, *24*, 9810–9823.
[24] M. L. García Fernández, I. K. Levy, D. Salustro, R. M. Negri, L. M. Saleh Medina, *J. Polym. Environ.* **2024**, *32*, 3179–3194.
[25] A. D. Nascimento Porto Neto, C. F. D. Santos Cruz, M. R. Serafini, P. Dos Passos Menezes, Y. M. B. G. de Carvalho, C. R. S. Matos, P. S. Nunes, J. C. Cardoso, R. L. C. de Albuquerque Júnior, P. J. Rolim Neto, F. A. Silva, A. A. de Souza Araújo, *J. Therm. Anal. Calorim.* **2017**, *127*, 1707–1713.
[26] B. Gieroba, M. Krysa, K. Wojtowicz, A. Wiater, M. Pleszczyńska, M. Tomczyk, A. Sroka-Bartnicka, *Int. J. Mol. Sci.* **2020**, *21*, 3811.
[27] A. Rafati, K. Tahvildari, M. Nozari, *Energy Sources, Part A: Recovery, Utilization, and Environmental Effects* **2019**, *41*, 1062–1074.
[28] R. Ma, Y. Wang, H. Qi, C. Shi, G. Wei, L. Xiao, Z. Huang, S. Liu, H. Yu, C. Teng, H. Liu, V. Murugadoss, J. Zhang, Y. Wang, Z. Guo, *Composites, Part B* **2019**, *167*, 396–405.
[29] E. Wiercigroch, E. Szafraniec, K. Czamara, M. Z. Pacia, K. Majzner, K. Kochan, A. Kaczor, M. Baranska, K. Malek, *Spectrochim. Acta, Part A* **2017**, *185*, 317–335.
[30] a) A. Chami Khazraji, S. Robert, *J. Nanomater.* **2013**, *2013*, 409676; b) F. Abasalizadeh, S. V. Moghaddam, E. Alizadeh, E. akbari, E. Kashani, S. M. B. Fazljou, M. Torbati, A. Akbarzadeh, *J. Biol. Eng.* **2020**, *14*, 8.
[31] L. Motelica, D. Ficai, O.-C. Oprea, A. Ficai, V.-L. Ene, B.-S. Vasile, E. Andronescu, A.-M. Holban, *Nanomaterials* **2021**, *11*, 2377.

Manuscript received: January 24, 2025

© 2025 The Author(s). ChemistrySelect published by Wiley-VCH GmbH